

## **Supporting Information**

# **Selective permeabilization of Gram-negative bacterial membranes using multivalent peptide constructs for antibiotic sensitization**

### **Authors:**

Leslie W. Chan<sup>1</sup>, Kelsey E. Hern<sup>2</sup>, Chayanon Ngambenjawong<sup>2</sup>, Katie Lee<sup>3</sup>, Ester J. Kwon<sup>1</sup>, Deborah T. Hung<sup>3-5</sup>, Sangeeta N. Bhatia<sup>1-3,6-8\*</sup>

### **Affiliations:**

1. Koch Institute for Integrative Cancer Research, Massachusetts Institute of Technology, Cambridge, Massachusetts 02139, United States
2. Institute for Medical Engineering and Science, Massachusetts Institute of Technology, Cambridge, Massachusetts 02139, United States
3. Broad Institute of Massachusetts Institute of Technology and Harvard, Cambridge, Massachusetts 02139, United States
4. Department of Molecular Biology, Center for Computational and Integrative Biology, Massachusetts General Hospital, Boston, Massachusetts 02114, United States
5. Department of Genetics, Harvard Medical School, Boston, Massachusetts 02115, USA
6. Department of Electrical Engineering and Computer Science, Massachusetts Institute of Technology, Cambridge, Massachusetts 02139, United States
7. Department of Medicine, Brigham and Women's Hospital, Harvard Medical School, Boston, Massachusetts 02115, United States
8. Howard Hughes Medical Institute, Cambridge, Massachusetts 02139, United States

\*Corresponding Author: Sangeeta N. Bhatia

Address: 500 Main Street, 76-453, Cambridge, MA 02142, USA

Phone: 617-253-0893

Fax: 617-324-0740

Email: [sbhatia@mit.edu](mailto:sbhatia@mit.edu)

## **Table of Contents**

Table S1. Candidate peptides for peptide-antibiotic conjugates	Pgs. S3-S4
Table S2. MIC values for peptide-linezolid mixtures	Pg. S5
Table S3. Test reaction conditions for amine-functionalization of dextrans	Pg. S6
Table S4. Class, clinical breakpoints, and physicochemical properties of drugs in the tested antibiotic panel	Pgs. S7-S12
Figure S1. Synthetic scheme of azido-LZDvar	Pg. S13
Figure S2. Quantification of conjugated WLBU2 peptides in potentiator candidates	Pg. S14
Figure S3. FIC graphs for antibiotics in combination with WD40 in PA14	Pgs. S15-S16
Figure S4. FIC graphs for fusidic acid, clindamycin, and rifampin in combination with WD40 in clinical isolates	Pg. S17
References	Pgs. S18-S19

**Table S1.** Candidate peptides for peptide-antibiotic conjugates. D-amino acids are prefixed with d and in parenthesis. A cysteine was added to the C-terminal of each peptide for conjugation to linezolid-C<sub>6</sub>-azide.

Peptide	Sequence	Structure	Cell penetration/membrane disruption mechanism
Buforin 2	TRSSRAGLQFPVGRVHRLLRK	N-terminal random coil region (residues 1-4), an extended helical region (residues 5-10), a proline hinge (residue 11), and a C-terminal $\alpha$ -helical region (residues 12-21) <sup>1</sup>	<b>Transient toroidal pore formation;</b> penetrates membrane without permeabilization; removal of proline hinge causes peptide localization to the cell surface and membrane permeabilization <sup>2</sup>
Lactoferrin (Human)	KCFQWQRNMRKV RGPPVSCIKR	N-terminal amphipathic helix connected to a $\beta$ -strand via a loop; no disulfide bond included for linezolid screen <sup>3</sup>	Bacterial membrane depolarization via unknown mechanism <sup>3</sup>
LL-37	LLGDFFRKSK EKIGKEFKRIVQRIKDFLRNLVPRTES	Amphipathic $\alpha$ -helical peptide <sup>4</sup>	Forms oligomers in membranes; evidence suggest membrane disruption by peptide “carpeting” in the membrane or toroidal pore formation <sup>4</sup>
Pexiganan	GIGKFLKKAKKFGKAFVKILKK	Unstructured in solution; forms dimeric antiparallel $\alpha$ -helical coiled-coil structure upon association with lipid membranes <sup>5</sup>	Disrupts membrane through <b>toroidal-type pore formation</b> <sup>5</sup>
PR-26	RRRPRPPYLPRPRPPPFFPPRLPPRI	Extended <sup>6</sup>	Antimicrobial domain of the cathelicidin PR-39, previously shown to translocate via an <b>inner membrane transporter</b> SbmA; non-lytic transport mechanism <sup>7</sup>
S4 <sub>13</sub> -PV	ALWKTLLKKVLKAPKKKRKV	Unstructured in solution <sup>8</sup>	Undergoes conformational change into helix during interaction with membrane <sup>8</sup>

TAT	YGRKKRRQRRRG	Random coil <sup>9</sup>	<b>Carpet model of membrane disruption<sup>9</sup></b>
WLBU2	RRWVRRVRRWVRRVVVRWVRR	Amphipathic $\alpha$ -helical peptide <sup>10</sup>	Proposed mechanism: <b>domain formation</b> with different elasticity that leads to leakage along domain walls <sup>11</sup>
4D-K <sub>5</sub> L <sub>7</sub>	KL(dL)(dL)KLK(dL)K(dL)LK	Amphipathic $\alpha$ -helical peptide <sup>12</sup>	Inserts into membrane and induces LPS miscellization; <b>carpet and detergent model of membrane disruption<sup>12</sup></b>

**Table S2.** MIC values for peptides alone and physical mixtures of peptides with a fixed concentration of linezolid (80  $\mu$ M). Values were determined via microdilution assays with *P. aeruginosa* (strain PA14).

Peptide	MIC	$\text{MIC}_{+\text{LZD}}$
Buforin 2	10	10
Lactoferrin	>40	>40
LL-37	20	20
Pexiganan	1.25	1.25
PR-26	5	5
S4 <sub>13</sub> -PV	2.5	2.5
TAT	>40	>40
WLBU2	>40	>40
4D-K <sub>5</sub> L <sub>7</sub>	10	10

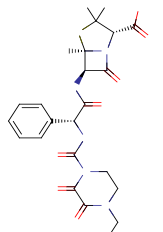
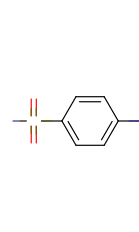
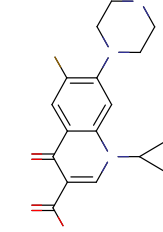
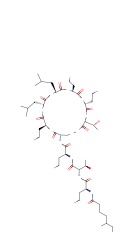
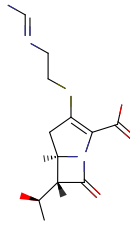
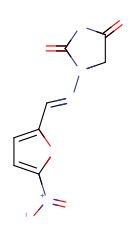
**Table S3.** Test reaction conditions for amine-functionalization of 0.5-g dextran quantities.

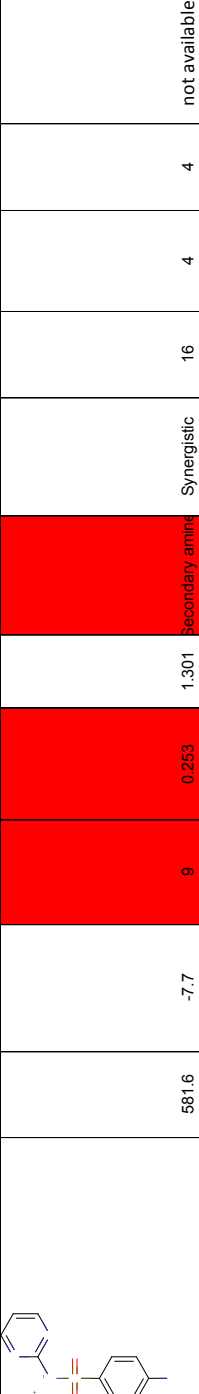
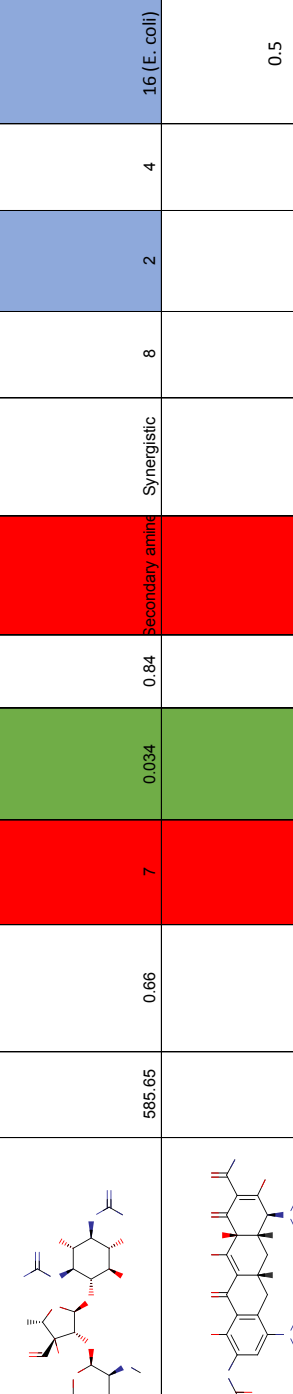
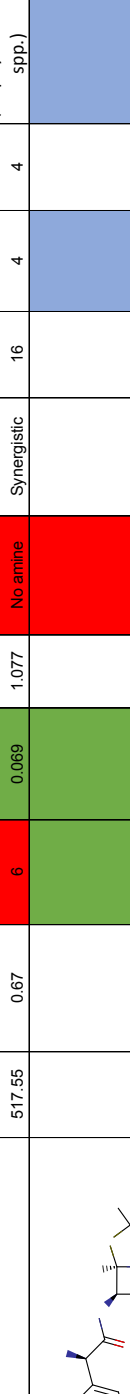
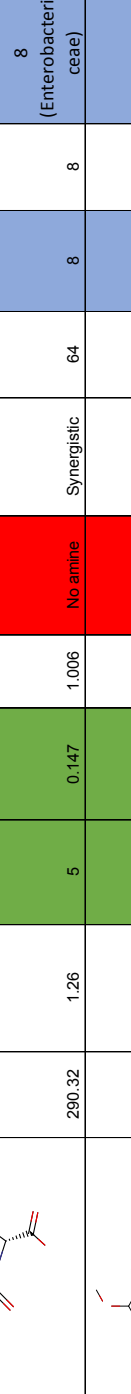
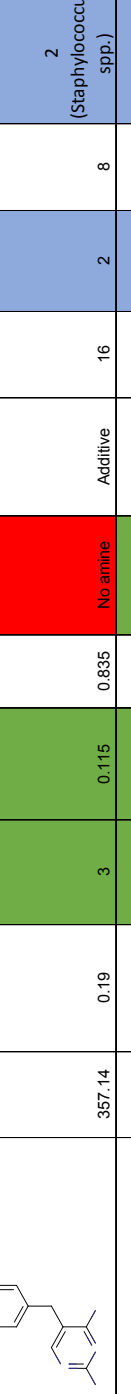
\*Indicates dextrans used to make WD10 and WD40 potentiator candidates.

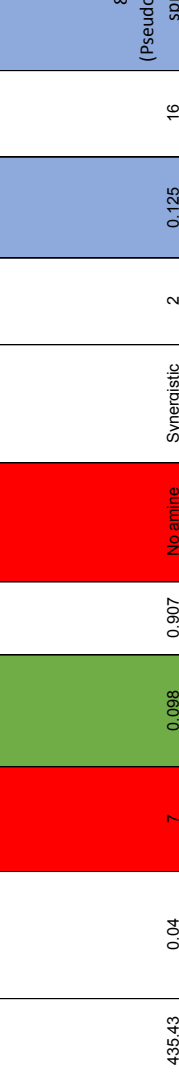
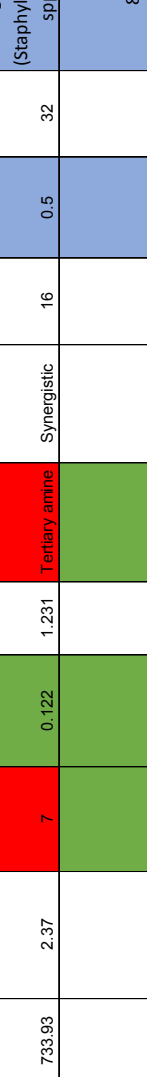
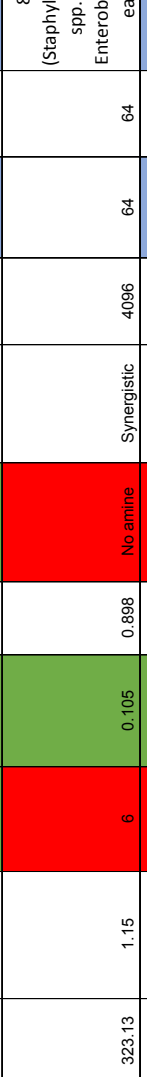
Sample ID	Dextran MW	Molar ratio sodium periodate: dextran	mL 100 mM sodium periodate	mL 3 M ethylenediamine (in 0.1 M sodium phosphate buffer, pH 7.4, 150 mM NaCl)	mL 1 M cyanoborohydride	Amine groups per dextran
Am-Dex10-100	10 kDa	12.5:1	18.75	12.5	2.5	5
<b>Am-Dex10-200*</b>	<b>10 kDa</b>	<b>25:1</b>	<b>12.5</b>	<b>12.5</b>	<b>2.5</b>	<b>27</b>
Am-Dex10-300	10 kDa	37.5	6.25	12.5	2.5	40
<b>Am-Dex40-100*</b>	<b>40 kDa</b>	<b>50:1</b>	<b>18.75</b>	<b>12.5</b>	<b>2.5</b>	<b>22</b>
Am-Dex40-200	40 kDa	100:1	12.5	12.5	2.5	34
Am-Dex40-300	40 kDa	150:1	6.25	12.5	2.5	70

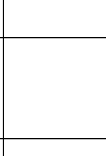
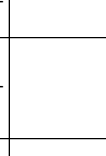
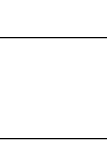
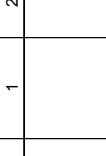
**Table S4. Class, clinical breakpoints, and physicochemical properties of drugs in the tested antibiotic panel.** Antibiotics with antipseudomonal activity are indicated with \*. Information for rotatable bonds, globularity, PBF, and functional groups were consolidated using ENTRYway (entry-way.org). Green indicates values that fall within favorable range for intracellular accumulation as defined by Richter et al. while red indicates those that do not. Yellow indicates values for antimicrobial peptides, which were excluded from correlation analyses. Clinical breakpoints were consolidated from CLSI or EUCAST. Blue indicates MIC values in the presence of WDF40 fall at or below the clinical breakpoint.

ANTIBIOTIC (Drug class; drug target)	Structure	MW	ClogP (ChemAxon)	Rotatable bonds	Globularity	PBF	Functional group	Activity with potentiator	MIC ( $\mu\text{g/mL}$ )	MIC <sub>w/o40</sub> ( $\mu\text{g/mL}$ )	MIC fold change	Clinical breakpoint ( $\mu\text{g/mL}$ )
<b>GENTAMICIN*</b> (Aminoglycoside; protein synthesis)		477.6	-3.1	7	0.069	1.085	Primary amine	Additive	1	1	1	4 ( <i>Pseudomonas</i> spp.)
<b>KANAMYCIN*</b> (Aminoglycoside; protein synthesis)		484.5	-3.1	6	0.122	1.169	Primary amine	Additive	32	32	1	1 ( <i>Pseudomonas</i> spp.)
<b>LEVOFLOXACIN*</b> (Fluoroquinolone; nucleic acid synthesis)		361.37	-0.02	2	0.048	0.655	Tertiary amine	Additive	0.5	0.5	1	1 ( <i>Pseudomonas</i> spp.)
<b>MEROPENEM*</b> (Carbapenem; cell wall)		383.46	-0.69	5	0.058	0.855	Secondary amine	Additive	0.5	0.25	2	2 ( <i>Pseudomonas</i> spp.)

								16 (Pseudomonas spp.)
238.16	0.03	3	0.079	0.616	No amine	Additive	4	2
								
172.2	-0.16	1	0.083	0.478	No amine	Additive	2048	1024
								
331.34	-0.57	3	0.04	0.536	Secondary amine	Additive	0.25	0.0625
								
1155.45	0.22	28	NA	NA	Primary amine	Synergistic	1	0.25
								
299.35	-0.19	6	0.176	0.915	No amine	Additive	0.5	0.125
								
138.06	-0.86	1	0.143	0.504	No amine	Synergistic	512	128
								4 (S. aureus)

	SILVER SULFADIAZINE (Sulfa antibiotics; cell wall)	581.6	-7.7	9	0.253	1.301	Secondary amine	Synergistic	16	4	4	not available
	STREPTOMYCIN* (Aminoglycoside; protein synthesis)	585.65	0.66	7	0.034	0.84	Secondary amine	Synergistic	8	2	4	16 (E. coli)
	TIGECYCLINE (Glycylcycline; protein synthesis)	517.55	0.67	6	0.069	1.077	No amine	Synergistic	16	4	4	0.5 (Staphylococcus spp.)
	AMPICILLIN (Beta-lactam; cell wall)	290.32	1.26	5	0.147	1.006	No amine	Synergistic	64	8	8	8 (Enterobacteriaceae)
	TRIMETHOPRIM (DHFR inhibitor; folate pathway)	357.14	0.19	3	0.115	0.835	No amine	Additive	16	2	8	2 (Staphylococcus spp.)
	AZTREONAM* (Beta-lactam monobactam; cell wall)	349.4	0.88	4	0.098	1.016	Primary amine	Synergistic	4	0.25	16	1 (Pseudomonas spp.)

 <b>CEFTAZIDIME*</b> (Beta-lactam: cell wall)	435.43	0.04	7	0.098	0.907	No amine	Synergistic	2	0.125	16	8 (Pseudomonas spp.)
 <b>DOXYCYCLINE</b> (Tetracycline: protein synthesis)	444.43	-0.72	2	0.206	1.178	Tertiary amine	Synergistic	64	2	32	1 (Staphylococcus spp.)
 <b>ERYTHROMYCIN</b> (Macrolide: protein synthesis)	546.58	-1.2	9	0.07	1.108	No amine	Synergistic	128	4	32	1 (Staphylococcus spp.)
 <b>FOSFOMYCIN</b> (Phosphonic acid: cell wall)	733.93	2.37	7	0.122	1.231	Tertiary amine	Synergistic	16	0.5	32	32 (Staphylococcus spp.)
 <b>AMOXICILLIN</b> (Beta-lactam: cell wall)	365.4	0.75	4	0.154	1.218	Primary amine	Synergistic	128	2	64	8 (Enterobacteriaceae)
 <b>CHLORAMPHENICOL</b> (Nitrobenzenes: protein synthesis)	323.13	1.15	6	0.105	0.898	No amine	Synergistic	4096	64	64	8 (Staphylococcus spp. and Enterobacteriaceae)
 <b>CLARITHROMYCIN</b> (Macrolide: protein synthesis)	747.95	3.18	8	0.191	1.359	Tertiary amine	Synergistic	128	2	64	2 (Staphylococcus spp.)

<b>LINEZOLID</b> (Oxazolidinone: protein synthesis)		337.35	0.61	4	0.067	0.939	No amine	4 (Staphylococcus spp.)
<b>NALIDIXIC ACID</b> (Quinolone: nucleic acid synthesis)		232.24	0.96	2	0.053	0.475	No amine	2 (Staphylococcus spp.)
<b>VANCOMYCIN</b> (Glycopeptide: cell wall)		1449.3	1.11	13	NA	NA	Primary amine	2 (Staphylococcus spp.)
<b>NOVOBIOCIN</b> (Aminocoumarin: nucleic acid synthesis)		612.62	3.07	9	0.04	1.114	No amine	2 (Staphylococcus spp.)
<b>RETAPAMULIN</b> (Peptormulin: protein synthesis)		517.76	4.63	6	0.105	1.226	Tertiary amine	2 (Staphylococcus spp.)
<b>MUPIRCIN</b> (Carboxylic acid: protein synthesis)		500.62	2.25	17	0.04	1.124	No amine	1 (Staphylococcus spp.)

<b>FUSIDIC ACID</b> (Fusidane; protein synthesis)	516.71	4.97	6	0.21	1.428	No amine
<b>RIFAMPIN</b> (Antimycobacterial; nucleic acid synthesis)	822.94	3.85	5	0.256	1.841	Tertiary amine
<b>CLINDAMYCIN</b> (Lincosamide; protein synthesis)	424.98	1.59	7	0.101	1.108	Tertiary amine

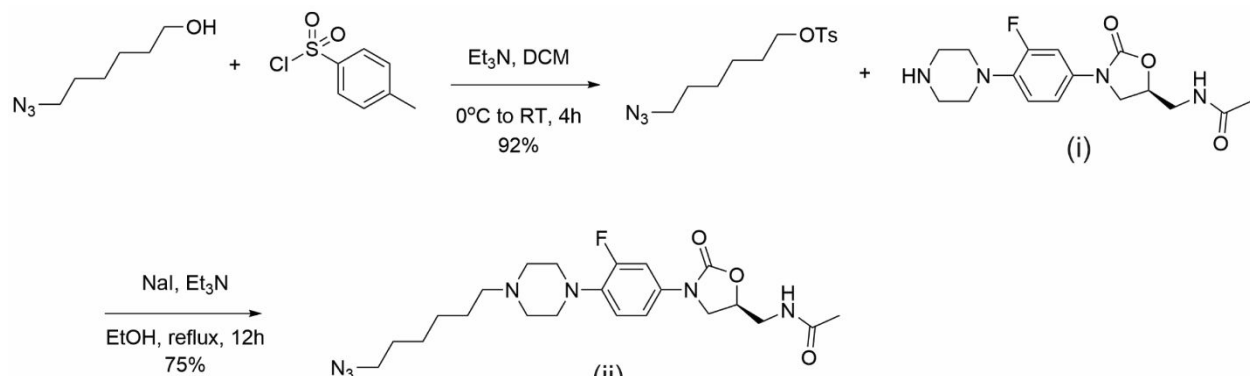


**Figure S1. Synthetic scheme for azido-functionalized linezolid variant (Azido-LZDvar, compound ii).** In this synthetic pathway, a piperazine variant of linezolid (compound i) is alkylated with a C<sub>6</sub>-azide linker using reaction conditions previously reported by Phetsang et al.<sup>13</sup>

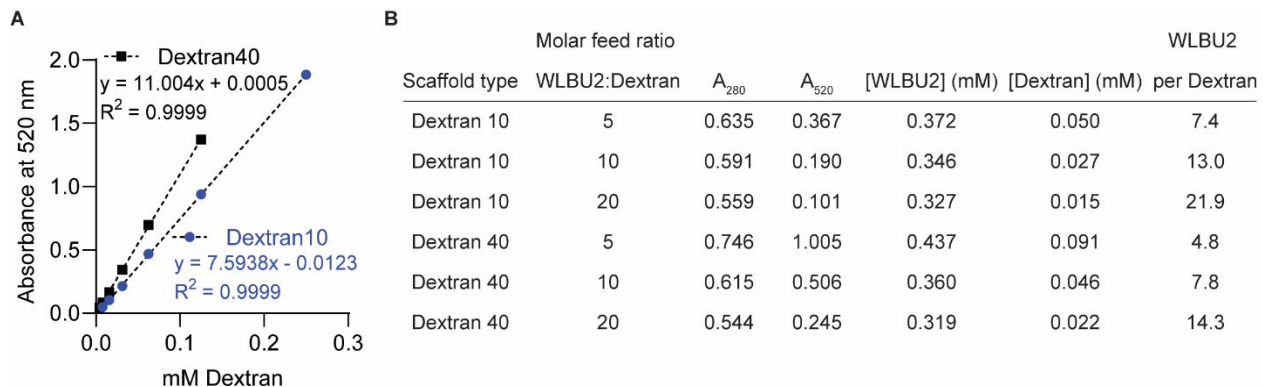


**Figure S2. Quantification of conjugated WLBU2 peptides in potentiator candidates.**

WLBU2 peptides were conjugated onto rhodamine-labelled Dextran 10 and Dextran 40. **(A)** Standard curves were generated via measurement of absorbance at 520 nm wavelength for serially-diluted solutions containing known concentrations of rhodamine-labelled Dextran 10 and Dextran 40 in PBS. **(B)** 3 different molar feed ratios (5, 10, or 20 WLBU2 peptides to dextran) were used per scaffold type to generate 6 potentiator candidates. After purification and lyophilization, dried samples were dissolved in PBS and absorbance at 280 nm and 520 nm wavelength were used to calculate molar concentrations of WLBU2 peptide and dextrans, respectively. Beer's Law,  $A = \epsilon cl$ , was used to convert absorbance to peptide concentration ( $A = A_{280}$ ,  $\epsilon_{WLBU2} = 17,070 \text{ M}^{-1}\cdot\text{cm}^{-1}$ ,  $l = 0.1\text{cm}$ ). Equations for the standard curves shown in **(A)** were used to convert absorbance at 520 nm ( $A_{520}$ ) to dextran concentration.

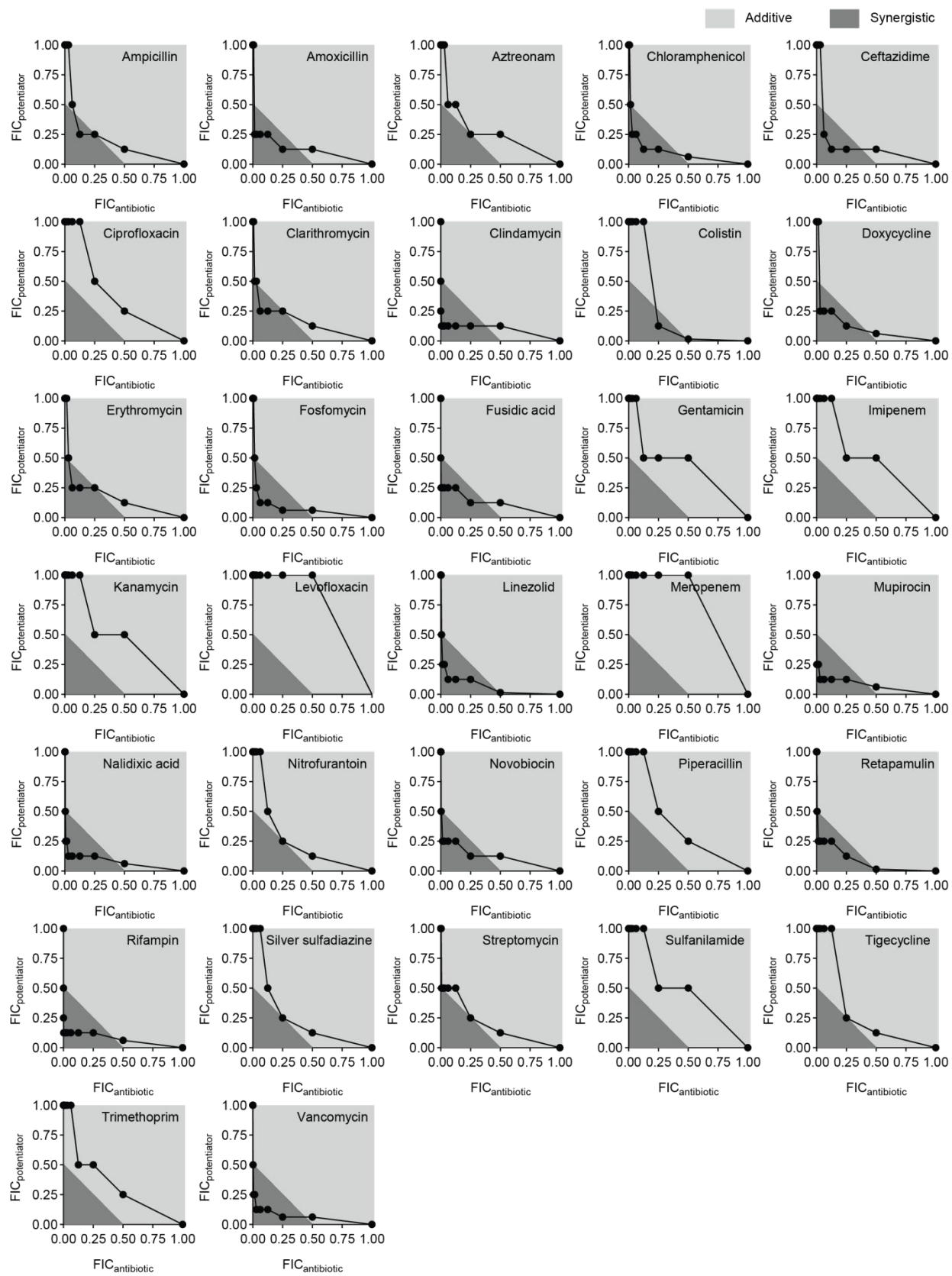


**Figure S3.** FIC values from checkerboard assays to characterize the activity of different antibiotics in combination with the WD40 in PA14.

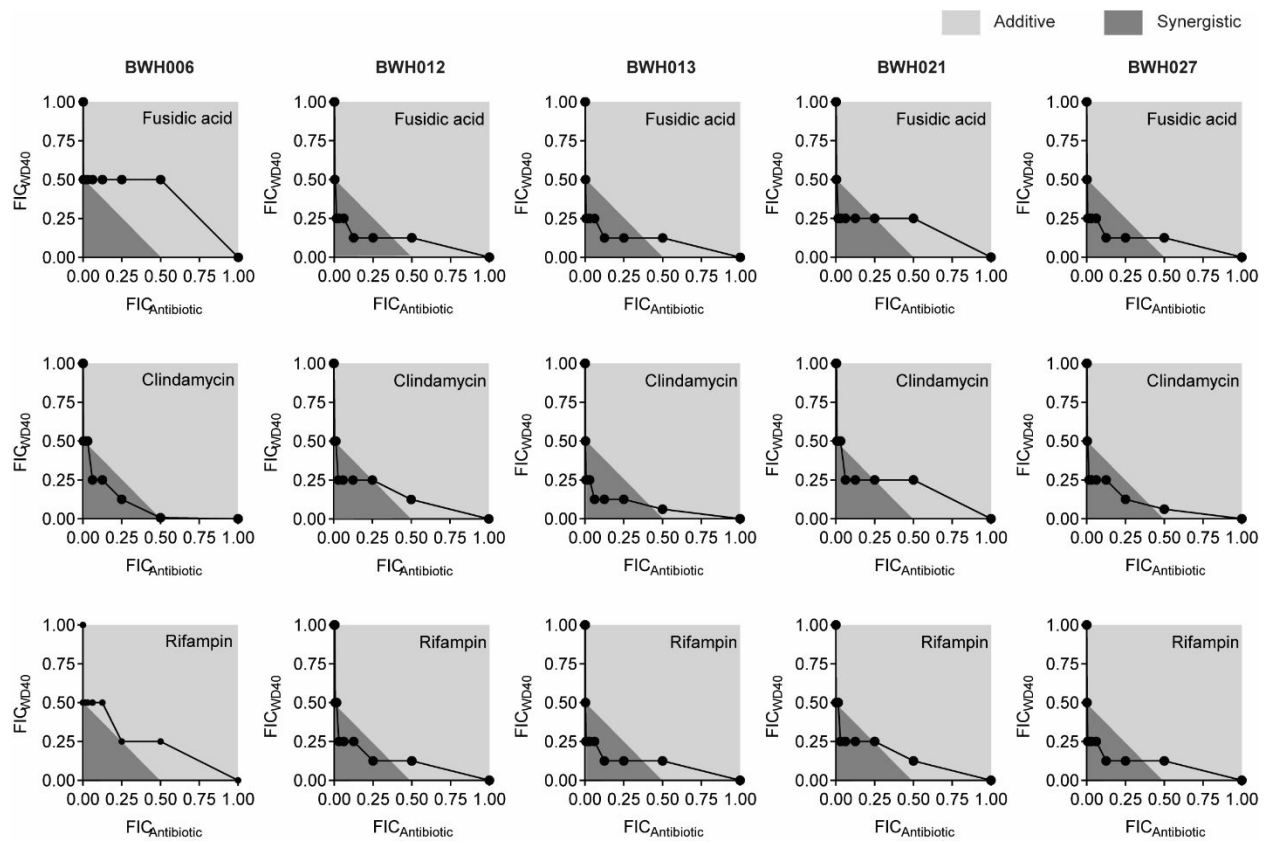


**Figure S4.** FIC values from checkerboard assays to characterize the activity of fusidic acid, clindamycin, and rifampin in combination with WD40 in clinical isolates BWH006, BWH012, BWH013, BWH021, and BWH027.

## Supplementary References

- (1) Park, C. B.; Yi, K. S.; Matsuzaki, K.; Kim, M. S.; Kim, S. C. Structure-Activity Analysis of Buforin II, a Histone H2A-Derived Antimicrobial Peptide: The Proline Hinge Is Responsible for the Cell-Penetrating Ability of Buforin II. *Proc. Natl. Acad. Sci. U. S. A.* **2000**, *97* (15), 8245–8250. <https://doi.org/10.1073/pnas.150518097>.
- (2) Kobayashi, S.; Chikushi, A.; Tougu, S.; Imura, Y.; Nishida, M.; Yano, Y.; Matsuzaki, K. Membrane Translocation Mechanism of the Antimicrobial Peptide Buforin 2. *Biochemistry* **2004**, *43* (49), 15610–15616. <https://doi.org/10.1021/bi048206q>.
- (3) Sinha, M.; Kaushik, S.; Kaur, P.; Sharma, S.; Singh, T. P. Antimicrobial Lactoferrin Peptides: The Hidden Players in the Protective Function of a Multifunctional Protein. *Int. J. Pept.* **2013**, *2013*. <https://doi.org/10.1155/2013/390230>.
- (4) Dürr, U. H. N.; Sudheendra, U. S.; Ramamoorthy, A. LL-37, the Only Human Member of the Cathelicidin Family of Antimicrobial Peptides. *Biochim. Biophys. Acta - Biomembr.* **2006**, *1758* (9), 1408–1425. <https://doi.org/10.1016/j.bbamem.2006.03.030>.
- (5) Hallock, K. J.; Lee, D. K.; Ramamoorthy, A. MSI-78, an Analogue of the Magainin Antimicrobial Peptides, Disrupts Lipid Bilayer Structure via Positive Curvature Strain. *Biophys. J.* **2003**, *84* (5), 3052–3060. [https://doi.org/10.1016/S0006-3495\(03\)70031-9](https://doi.org/10.1016/S0006-3495(03)70031-9).
- (6) Cardoso, M. H.; Meneguetti, B. T.; Costa, B. O.; Buccini, D. F.; Oshiro, K. G. N.; Preza, S. L. E.; Carvalho, C. M. E.; Migliolo, L.; Franco, O. L. Non-Lytic Antibacterial Peptides That Translocate through Bacterial Membranes to Act on Intracellular Targets. *Int. J. Mol. Sci.* **2019**, *20* (19). <https://doi.org/10.3390/ijms20194877>.
- (7) Mattiuzzo, M.; Bandiera, A.; Gennaro, R.; Benincasa, M.; Pacor, S.; Antcheva, N.; Scocchi, M. Role of the Escherichia Coli SbmA in the Antimicrobial Activity of Proline-Rich Peptides. *Mol. Microbiol.* **2007**, *66* (1), 151–163. <https://doi.org/10.1111/j.1365-2958.2007.05903.x>.
- (8) Mano, M.; Henriques, A.; Paiva, A.; Prieto, M.; Gavilanes, F.; Simoes, S.; de Lima, P. Cellular Uptake of S413-PV Peptide Occurs upon Conformational Changes Induced by Peptide-Membrane Interactions. *Biochim. Biophys. Acta* **2006**, *1758*, 336–346.
- (9) Eiríksdóttir, E.; Konate, K.; Langel, Ü.; Divita, G.; Deshayes, S. Secondary Structure of Cell-Penetrating Peptides Controls Membrane Interaction and Insertion. *Biochim. Biophys. Acta - Biomembr.* **2010**, *1798* (6), 1119–1128. <https://doi.org/10.1016/j.bbamem.2010.03.005>.
- (10) Deslouches, B.; Phadke, S. M.; Lazarevic, V.; Cascio, M.; Ismal, K.; Montelaro, R. C.; Mietzner, T. A. De Novo Generation of Cationic Antimicrobial Peptides: Influence of Length and Tryptophan Substitution on Antimicrobial Activity. *Antimicrob. Agents Chemother.* **2005**, *49* (1), 316–322. <https://doi.org/10.1128/AAC.49.1.316>.
- (11) Kumagai, A.; Dupuy, F. G.; Arsov, Z.; Elhady, Y.; Moody, D.; Ernst, R. K.; Deslouches, B.; Montelaro, R. C.; Di, Y. P.; Tristam-Nagle, S. Elastic Behavior of Model Membranes with Antimicrobial Peptides Depends on Lipid Specificity and D-Enantiomers. *Soft Matter* **2019**, *15* (8), 1860–1868. <https://doi.org/10.1039/c8sm02180e.Elastic>.
- (12) Papo, N.; Shai, Y. A Molecular Mechanism for Lipopolysaccharide Protection of Gram-Negative Bacteria from Antimicrobial Peptides. *J. Biol. Chem.* **2005**, *280* (11), 10378–10387. <https://doi.org/10.1074/jbc.M412865200>.

- (13) Phetsang, W.; Blaskovich, M. A. T.; Butler, M. S.; Huang, J. X.; Zuegg, J.; Mamidyala, S. K.; Ramu, S.; Kavanagh, A. M.; Cooper, M. A. Bioorganic & Medicinal Chemistry An Azido-Oxazolidinone Antibiotic for Live Bacterial Cell Imaging and Generation of Antibiotic Variants. *Bioorg. Med. Chem.* **2014**, 22 (16), 4490–4498.  
<https://doi.org/10.1016/j.bmc.2014.05.054>.